Cluster-oriented Detection of Microcalcifications in Simulated Low-Dose Mammography

Hartmut Führ[1], Oliver Treiber[1] and Friedrich Wanninger[2]

GSF Forschungszentrum für Umwelt und Gesundheit
[1] Institut für Biomathematik und Biometrie
[2] Institut für Strahlenschutz
Ingolstädter Landstraße 1, D-85764 Oberschleißheim
Email: fuehr@gsf.de

Abstract. The problem of assessing the potential for dose reduction in X-ray mammography has been addressed in the paper [1] via numerical simulation, using the detection of microcalcifications as a benchmark to measure the loss of image quality in the dose-reduced images. In this paper we present an extension of the original algorithm, which prefers clusters over single microcalcifications, and show test results indicating that the modification makes the algorithm more robust with respect to the image degradations due to dose reduction.

1 Introduction

The large numbers of participants in mammography screening programmes render the issues of radiation dose and the potential for dose reduction particularly relevant. This observation provided the initial motivation for a project carried out at GSF, which had the aims of simulating and assessing the effect of dose reduction on image quality.

The importance of microcalcifications as diagnostic indicators for mammacarcinomae in X-ray mammography suggests using the detection of microcalcifications as a natural benchmark problem to measure the loss of image quality due to dose reduction. We thus developed and implemented an algorithm for the detection of microcalcifications, and evaluated its performance on real and dose-reduced images by use of FROC- and ROC-curves, for single microcalcifications and for clusters. The comparison of the various (F)ROC-curves allowed a first assessment of the potential for dose reduction and the critical parameters which control this problem. In the following we first give a short summary of the algorithm and the main results of the discussion in [1]. We then present a cluster-oriented modification of the algorithm and show evidence that this modification makes the algorithm more robust with respect to the image degradations due to dose reduction. The results presented here and in [1] should be understood as a case study, which could be also be carried out for other constellations of equipment.

2 Methods

The original motivation for the project was to address several related problems: To simulate the effects of dose reduction on X-ray images, to provide a method of measuring the loss in image quality due to dose reduction, and finally to develop image processing algorithms which could cope with this loss. The first two problems are discussed in [1], while in this paper we study a possible solution to the third one, i.e., a modification of the original algorithm designed to make it more robust with respect to dose reduction.

Both problems require a pool of test images. For this purpose a set of 25 patient images, containing microcalcifications on various textural backgrounds, were digitized. The original images were taken using of a SIEMENS MAMMOMAT 3000 with a KODAK Min-R 2000/2190 film-screen system, and digitized with a TANGO high resolution drum scanner, which resulted in a pixel size of $20\mu m$. The image degradations due to dose reduction were simulated numerically, based on certain model assumptions. The following two subsections contain a summary of the simulation and detection parts of [1]; a detailed description can be found in the paper.

2.1 Simulating Dose Reduction

It is obvious that a decrease in dose results in a loss of contrast. Therefore, dose reduction will only be feasible if the film/screen-system makes up for this by a more effective conversion of incident quantum fluence to gray value. It is reasonable to expect that this additional efficiency is bought at the price of lower image resolution, which could result either from changes in the film or in the scintillator screen. In terms of the modelling, the additional smoothing is described by the new film/screen modulation transfer function, which will be lower than that of the original system. A second feature which needs to be modelled is the amount and appearance of the noise contained in the image. Hence numerical simulation of dose reduction consists of two steps: First a smoothing of the original image which takes into account the lower MTF of the new system, and then adding suitably scaled noise to ensure the correct noise level and noise spectra in the new image.

It should be emphasized that the model parameters describing the more sensitive film/screen system do not refer to any existing equipment, but are obtained by extrapolating the original parameters, given in [2]. We have simulated two models for the more sensitive film/screen system, which differ in the amount of additional smoothing incurred by the new system. They are referred to in the following (as in [1]) by "moderately smoothing" and "strongly smoothing". Figure 1 gives a comparison of an original image ROI with two versions obtained by simulating 50 % dose reduction and moderate smoothing, and 25 % dose reduction with strong smoothing.

The test results revealed that the smoothing behaviour was crucial for the performance of the detection algorithm: In the moderately smoothing case, a dose reduction by 25 % did not entail any decrease of performance, while reducing

Fig. 1. Comparison of original image to dose-reduced version: ROI of size $5 \times 5mm^2$. The left image is the original, the middle image is obtained assuming a dose reduction of 50 % and moderate smoothing, whereas the image on the right is obtained for a dose reduction of 25 % and strong smoothing. There is a cluster of rather subtle microcalcifications in the lower right corner of the image which is increasingly less visible in the dose-reduced images.

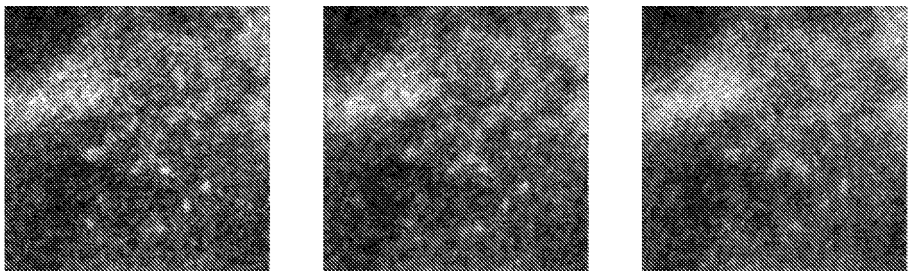

by 50 % did. For the strongly smoothing model, even 25 % dose reduction leads to a marked drop in detection rates.

2.2 Microcalcification Detection by Matched Filtering

The detection algorithm in [1] is based on a matched filtering approach, taking in account the noise spectra (taken from [2] for the original images, and extrapolated for the dose-reduced versions). Here the noise is modelled as locally stationary, with the local spectrum depending on a background image (assumed to be slowly varying). The matched filter is a Laplacian of Gaussian. The filter output is compared to the expected noise variance in the filtered image, as computed from the spectra and an estimate of the slowly varying background image. The quotient of filter output and variance estimate provides a "significance image", with large values pointing to probable locations of microcalcifications. Pixels are collected in connected regions using a region growing algorithm, which starts from local maxima of the significance image. As a result, we obtain two related pieces of data:

1. Subsets Ω_j $(j = 1, \ldots, N)$ of the image indicating suspicious regions.
2. For each region Ω_j the value s_j of the significance image at the seed point. This value is interpreted as a degree of suspiciousness; the larger s_j, the more suspicious Ω_j is of being a microcalcification.

The final detection step then consists in thresholding: Ω_j is declared a microcalcification if $s_j \geq T$, for a certain prescribed threshold T.

2.3 Cluster-Oriented Enhancement of the Detection Algorithm

We now describe the cluster-oriented strategy which is intended to enhance the algorithm performance. It amounts to preferring suspicious regions lying close

to other such regions. This can be achieved by in modifying the s_j prior to thresholding, by a factor ϕ_j which increases with the number of neighbours (however defined). Obviously there are many ways of making this explicit. We have chosen the following:

1. Fix a distance d and a threshold T.
2. Compute all regions Ω_j $j = 1, \ldots, N$ with $s_j \geq T/2$.
3. Declare two regions "near" whenever their seed points have a Euclidean distance of at most d. For each index $j \in \{1, \ldots, N\}$ define recursively the index sets I_n^j by letting $I_0^j = \{j\}$ and

$$I_{n+1}^j = \{i : \Omega_i \text{ and } \Omega_k \text{ are near for some } k \in I_n^j\} \ .$$

   This is obviously an increasing sequence of index sets, which stops growing after at most N steps. The cardinality $|I_N^j|$ is declared to be the number of neighbours of Ω_j.
4. Define

$$\widetilde{s}_j = s_j \cdot \phi(|I_N^j|) \ , \text{ where } \phi(m) = \frac{2m-1}{m}$$

5. Any region Ω_j with $\widetilde{s}_j \geq T$ is declared a microcalcification.

Our modifications are motivated by the following considerations:

1. The number of neighbours only has a limited influence since ϕ is bounded. Moreover, for regions with large numbers of neighbours their precise number is irrelevant: $\phi(n)$ increases sharply for small n and is more or less constant for large n.
2. All elements in a group of suspicious regions are reassessed in the same way, regardless of whether they are in the center of that group or at the periphery.

2.4 Test Procedure

We use the same database and test procedure as in [1]. The database consists of 51 patches of size $1 \times 1cm^2$ or 500×500 pixels. Each patch is divided into 4 subpatches of $5 \times 5mm^2$, and such a subpatch is declared to contain a cluster if it contains at least three microcalcifications. For a fixed parameter setting we obtain true positive and false positive rates, based on a comparison to ground truth markings obtained from the inspection of the original images by an experienced radiologist. Varying the threshold T, while fixing all other parameters, provides a means of visualising how the algorithm handles the tradeoff between suppression of false positives and detection of true positives, in the form of an ROC curve.

3 Results

Figure 2 gives a comparison of the detection results of the original algorithm versus the cluster-oriented version, on original images for 50 % dose reduction and moderate smoothing, and 25 % dose reduction and strong smoothing.

Fig. 2. Comparison of the ROC curves, for 50 % dose reduction and moderate smoothing (left hand side) and 25 % dose reduction and strong smoothing (right hand side). In both graphs, the symbol + marks the ROC curves computed for the original images and the original algorithm, and $*$ describes the performance of the cluster-oriented algorithm on the original images. The ROC curves for the dose-reduced images are marked by $\triangle$ (for the original algorithm) and $\diamond$ (cluster-oriented version).

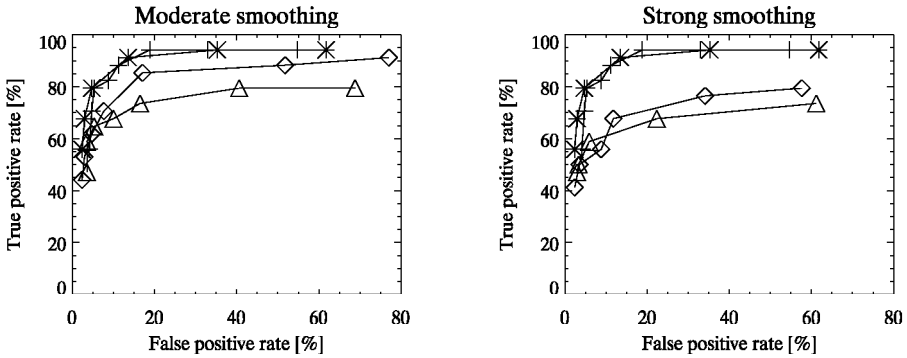

In all cases the cluster-oriented version uses precisely the same parameter set for the first detection step as the original algorithm. The distance d in the cluster-oriented part of the detection algorithm was chosen as $d = 100$. The plots show that the cluster-oriented algorithm does not yield any significant change in performance on the originals, but a clear improvement on the dose-reduced images, for all false positive rates in the moderately smoothing case, and for false positive rates ≥ 10 % in the strongly smoothing case. It is also plain from the plots that the improvement does not completely make up for the degradation in image quality.

Acknowledgements

We thank PD Dr. Sittek of Klinikum Großhadern for radiological advice, the set of test images and ground truth markings. T. Szygowski implemented the cluster-based extension of the detection algorithm. The project was in part funded by the HGF Strategiefond II, "Therapie und Diagnose von Mammakarzinomen".

References

1. Treiber OM, Wanninger F, Führ H, Panzer W, Regulla D, Winkler G: An adaptive algorithm for the detection of microcalcifications in simulated low-dose mammography. Physics in Medicine and Biology, to appear. Preprint version available under http://www.gsf.de/ibb/preprints.php.
2. Bunch PC: Advances in high-speed mammographic image quality Proc. SPIE Vol. 3659:120-130, 1999.